Mechanisms of Nonwetting Phase Trapping during Imbibition at Slow Rates

LI YU (Y. LI)* AND NORMAN CLAUDE WARDLAW†

*Nanhai Western Oil Company, Zanjiang, People's Republic of China, and †Department of Geology and Geophysics, University of Calgary, Calgary, Alberta T2N 1N4, Canada

Received February 22, 1985; accepted June 25, 1985

Experiments performed in transparent-glass micromodels were used to observe the mechanisms of both wetting phase (wp) and nonwetting phase (nwp) disconnection and entrapment during drainage and imbibition at slow rates. Convex and selloidal menisci, slowly advanced by an externally imposed flow during imbibition, periodically exceed limits of stability and undergo short, rapid advances during which nwp may become disconnected by one of two processes referred to as snap-off and break-off. Snap-off involves selloidal menisci and can occur within throats, within pores or at the junction region of pores and throats. Break-off refers to rupture during piston-type advance of a convex interface which contacts an opposing pore wall. The critical capillary pressures and other conditions for snap-off in throats, piston-type motions in pores, snap-off in pores and break-off have been determined experimentally and provide the basis for simulating microscopic displacement processes in media with any specified structure and wettability. These interface movements during imbibition are influenced by the sizes, shapes, and arrangement of both pores and throats with respect to the direction of advancing displacing phase. Earlier interface motions determine what is possible subsequently and the sequence and position of snap-off and break-off events determine the amount and location of trapped nonwetting phase. Wettability and topology are the main factors which determine whether snap-off occurs in throats, in pores, or at pore–throat junctions.

I. INTRODUCTION

Oil and gas reservoir rocks, and other types of porous media are three-dimensional networks composed of larger spaces (pores) connected through constrictions or smaller spaces (throats). Where these spaces are occupied by two immiscible fluids, one of which is wetting and the other nonwetting, for example, water and oil, displacement of nonwetting by wetting is referred to as imbibition and the reverse process is drainage. The advance of fluid interfaces during imbibition at slow rates is controlled primarily by capillary forces. Some of these interface movements break or disconnect previously continuous and flowing filaments of nonwetting phase which become immobile or "trapped," since only continuous filaments of fluid can flow during low capillary number displacements.

Experiments performed in transparent glass micromodels were used to observe the mechanisms and to define the conditions of both nonwetting fluid and wetting-fluid disconnection and entrapment on length scales equivalent to a few pore–throat lengths. The effects of pore–throat size, shape, connectivity, and arrangement (topology), in combination with the prevailing contact angle for fluid interfaces, determine the mechanism of disconnection and the amount and location of trapped fluid. Understanding the mechanisms and conditions of disconnection is the major purpose of this study. It is a necessary first step to more complex evaluations such as predicting the location and amount of residual fluid and to understanding the relationships of pore structure, wettability, and saturation to relative permeability and to drainage–imbibition capillary pressures.

Static menisci between two immiscible fluids in pores have shapes determined by local geometry and wettability and obey the Young–

0021-9797/86 $3.00

Laplace equation of capillary hydrostatics (1). However, menisci may be connected by other fluid interfaces which are separated from the solid only by thin films. Such interfaces do not adopt shapes predicted by the Young–Laplace equation (2, 3).

The Young–Laplace equation provides the relationship between capillary pressure (P_c), interfacial tension (γ) and two radii of curvature of a meniscus,

$$P_c = \gamma\left(\frac{1}{R_1} + \frac{1}{R_2}\right), \qquad [1]$$

where R_1 and R_2 are radii measured in planes at right angles to each other and containing a perpendicular to the meniscus surface. If R_1 and R_2 are on the same side of the interface we refer to the meniscus as convex and both curvatures are positive. Following terminology used by Lenormand and Zarcone (4), we refer to reversible motions of a convex meniscus as "piston-type" motions (Figs. 1A and E). Alternatively, a meniscus can be selloidal (saddle-shaped) and have components of positive and negative curvature with radii on opposite sides of the meniscus (Figs. 1B, C, D).

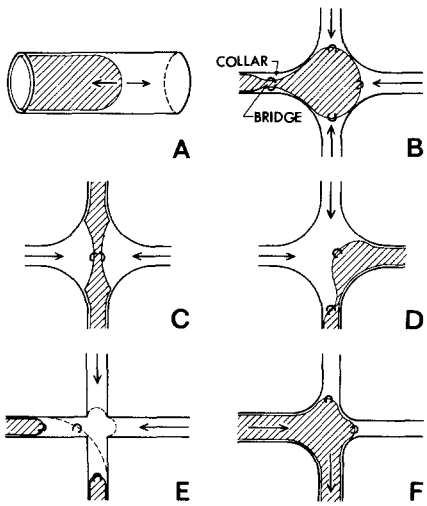

FIG. 1. Interface types and configurations A–E are for imbibition. Nonwetting phase shaded; (A) convex interface, piston-type advance and retreat; (B) selloidal interface, snap-off in throat; (C) selloidal interface, snap-off in pore; (D) selloidal interface, snap-off at pore–throat junction; (E) convex interface, break-off in pore; (F) drainage.

Convex and selloidal menisci slowly advanced by an externally imposed flow, periodically exceed limits of stability and undergo short, rapid advances to assume more stable configurations. During these unstable events, nonwetting phase (nwp) may become disconnected by one of two processes referred to as snap-off and break-off.

We refer to snap-off mainly in imbibition although snap-off also can occur during drainage (5). Snap-off always involves selloidal menisci and can occur within throats, within pores, or at the junction regions of pores and throats (Figs. 1B, C, and D, respectively). Wetting phase moves through thin wetting films or along small surface grooves or pits (surface roughness) (3) to a growing collar of wetting phase (wp). At a critical capillary pressure and finite value of the bridge radius (Fig. 1B), the interface becomes unstable and ruptures the nwp bridge. Two new interfaces are created which then may be able to move by piston-type motion.

Elsewhere (6), we have shown that for specific advancing contact angles (θ_A) and a fixed value of the pore (r_p)-to-throat (r_t) size ratio greater than a critical value (critical aspect ratio) snap-off in throats can occur at higher capillary pressures (P_{st}) than the capillary pressure (P_{pp}) for piston-type meniscus advance in the adjacent pores. Nonwetting phase continuity may be broken and nwp is trapped in the pore. As θ_A increases from 0° to ~55°, r_p/r_t increases from ~1.5 to ~1.75. For θ_A greater than about 70°, r_p/r_t becomes infinite and snap-off cannot occur in throats during quasistatic displacements. Assuming similar cross sectional shapes and wettabilities for pores and throats, "critical aspect ratio" (r_p/r_t) is an hypothetical minimum pore-to-throat size ratio which makes snap-off possible. It is equal to the ratio of the piston-type withdrawal capillary pressure for a throat (P_{pt}) to the snap-off capillary pressure *in the same throat* (P_{st}). That is, $r_p/r_t = P_{pt}/P_{st}$. We designate the "critical capillary pressure ratio" for snap-off in

throats (P_t^*) as $P_t^* = P_{pt}/P_{st}$. Thus, $r_p/r_t = P_{pt}/P_{pp} = P_{pt}/P_{st} = P_t^*$.

Although critical aspect ratio for snap-off in throats can be defined as either r_p/r_t or P_{pt}/P_{st}, whether snap-off can occur in a given throat also depends on other factors such as the connectivity of throats and pores and the continuity or otherwise of the immiscible fluid phases. Thus, the critical aspect ratio for a particular pore and its connecting throats is only one of several factors which determine whether or not nwp will be trapped in that pore.

The concept of snap-off *in pores* and at pore–throat junctions (Figs. 1C and D), as distinct from snap-off in throats, appears to have been neglected in the published literature. However, it is important to recognize the various sites at which snap-off can occur because, for the same pores and throats but for differing wettabilities, snap-off at different sites occurs at different capillary pressures. The ratio of the piston-type withdrawal capillary pressure for a pore (P_{pp}) to the snap-off capillary pressure *in the same pore* (P_{sp}) is the critical capillary pressure ratio for snap-off in pores (P_p^*), where $P_p^* = P_{pp}/P_{sp}$. P_p^* is ~ 1.5 for $\theta_A = 0°$ but decreases to 1.03 for $\theta_A > 20°$. P_p^* and P_t^* both are functions of cross-sectional shape as well as wettability.

Mohanty *et al.* (3) use the term break-off for a pore body evacuation process in which a single interface becomes 2 or more interfaces as the result of a jump by an unstable meniscus. We adopt this term but restrict its use to convex interfaces which become unstable and, during a jump through a pore, become ruptured by contact with an opposing pore wall (Fig. 1E). Lenormand *et al.* (4) referred to such events as type I2 imbibition.

During slow imbibition in a uniformly wetted system, capillary pressure decreases and snap-off occurs in throats at specific capillary pressures related to throat size but can only occur if a continuous filament of nwp is present from the snap-off site to the nwp sink. Once a blob of nwp is completely surrounded by wp, no further snap-off or break-off is possible within the disconnected region except during mobilization at higher capillary numbers.

The arrangement and connectedness of pores and throats (topology), as well as wettability and aspect ratio, determine whether or not nwp is trapped by snap-off in throats, snap-off in pores, or snap-off at pore–throat junctions. For a given θ_A, a pore can have less than the critical aspect ratio with respect to all directly connected throats and yet trap nwp by snap-off in those throats. Thus, it is necessary to recognize the effects of topology when discussing trapping by snap-off.

In the case of snap-off in pores or at pore–throat junctions, the site of snap-off and the amount of trapping depends on the position as well as the size of the throats which are supplying wetting phase to the pore.

Snap-off in throats is a bond-disconnection process whereas snap-off in pores or at pore–throat junctions and break-off are all site-disconnection processes. Individual break-off or snap-off events do not necessarily cause nwp entrapment but, eventually, nwp is completely disconnected and trapped by these events. In the early stages of displacement there is a high probability that snap-off events facilitate nwp withdrawal by creating new convex interfaces which undergo further piston-type withdrawal. However, in the later stages, there is a high probability that snap-off events will completely disconnect and trap portions of nwp.

In drainage, which is only mentioned briefly here, the displaced phase is wetting and becomes "trapped" by a process which we refer to as drainage bypassing and is distinguished from the trapping mechanisms described for imbibition. Wetting phase "trapped" by drainage bypassing is not completely disconnected because wetting films persist on surfaces or are associated with surface roughness. Further increases of drainage capillary pressure may reduce wetting phase saturation as shown experimentally by Lai (7). During drainage, snap-off of nwp occurs if the interface advances through a throat into a relatively large pore. The drops of nwp caused by snap-off

TABLE I

Interface Curvature, Stability, and Mechanisms of nwp Disconnection

Interface curvature	Stability	Event causing nwp disconnection	Location of event	Greater or less than critical aspect ratio
Convex-curvature positive	Stable	None	—	
	Unstable	Break-off	Pore	Less
Selloidal-curvature positive and negative	Stable	None	—	
	Unstable	Snap-off	Pore	
			Pore–throat junction	
			Throat	Greater

eventually coalesce and connect with continuous nwp before the pore is completely filled. This pore size related process is therefore not a controlling factor and the drainage process can still be considered as bond (throat) controlled.

In Table I, we summarize the relationships among interface form, stability, process of disconnection, and critical aspect ratio.

II. MODEL STRUCTURE

Pore–throat systems were etched into glass plates with hydrofluoric acid using the technique described in McKellar and Wardlaw (8). Pores are of two styles, one with concave outer boundaries which are referred to as concave pores (pore B1 to E1, Fig. 2) and the other with convex outer boundaries referred to as convex pores (Fig. 3). These forms were chosen because pores in unconsolidated sediments are characteristically concave whereas those formed by dissolution following consolidation and cementation (secondary pores) can be convex. Pores and throats are identified by letter and number (Fig. 2) and their relative sizes indicated by numbers 1 (smallest) to 5 (largest) on Fig. 3. The relative sizes are the same for both models.

Models with the two pore types, concave and convex, were each constructed with two different aspect ratios to give a total of four models. Models referred to as having low aspect ratio were prepared by etching mirror images of the pores and throats into two plates and registering them so that all pores and throats coincided. Models referred to as high aspect ratio were made by etching pores and throats into one plate but pores only into the second plate. In all models, pores were registered on both plates which were then firmly clamped in a holding frame. The pore–throat systems are connected by throats to large etched troughs which are source and sink for fluids which were accessed through tubes connected to these regions. Fluid pairs and associated contact angles are given in Table II. Flexible tubes connected to source or sink can be raised or lowered to control pressure.

The width and depth of all pores and throats on the glass plates were measured. Width was measured using a microscope with a calibrated

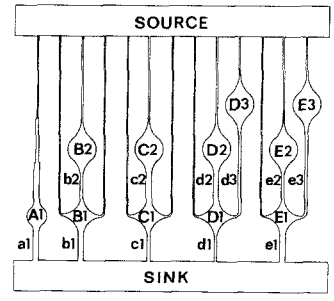

FIG. 2. Concave pore model. Pores and throats identified by upper case letters and numbers, and lower case letters and numbers, respectively.

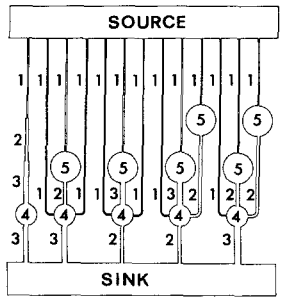

FIG. 3. Convex pore model. Relative sizes of all pores and throats indicated by numbers with 1 smallest and 5 largest.

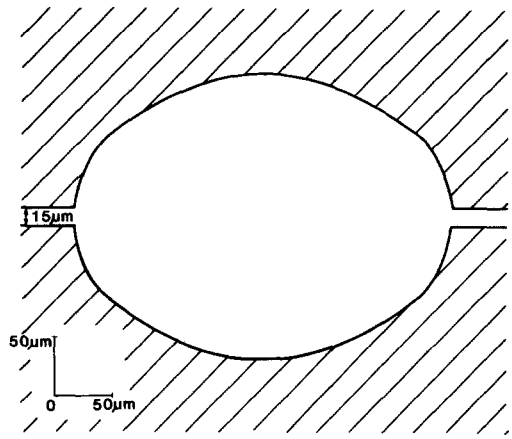

FIG. 4. Cross section of a throat etched into two glass plates.

micrometer disk in one of the oculars and depth was measured using a high-power objective with narrow depth of focus. The objective is focused first on the top surface of the glass and then at the bottom of the etched pores and throats. The fine focussing adjustment for the microscope stage is such that one small division corresponds approximately with a vertical change in position of 1 μm. The depth of etch varies from ~110 to 150 μm and a precision in measurement of about 1% of the depth could be attained. The depth of etch increases with width of throat or pore.

The vertical dimension of pores and throats includes a space of ~15 μm which is the average distance of separation of the clamped plates. This space is occupied by wetting fluid in all experiments. The lateral walls of pores and throats are not vertical and pores and throats are ellipsoidal in section (Fig. 4).

The widths of the largest and smallest concave and convex pores, measured as the diameters of maximum inscribed circles, are ~6.6 and ~4.5 mm, respectively. Throats have widths in three ranges: ~0.8–0.85, ~0.52–0.57, and 0.32–0.39 mm. All throats have lengths which are many times greater than widths (Figs. 2 and 3).

The measured average depths (y) and widths (x) for each pore and throat were converted to average effective diameters. The effective diameter (d_e) is the apparent diameter which satisfies the Young–Laplace equation

TABLE II

Contact Angles and Interfacial Tensions

Fluid pair and surface	Static (θ_I)	Advancing (θ_A)	Receding (θ_R)	Interfacial tension (γ) (mN/m)
Water–air, clean glass	0	0	0	72
Hexadecane–water, coated glass	23	24	22	36
Air–mercury, clean glass	45	48	43	485 (Ref. (10))
Pyridine + water–air, coated glass	63	68	57	54

Note. Contact angles are measured in the wetting phase and the first of the fluid pairs in the table is the wetting phase.

$$P_p = P_{nw} - P_w = \frac{4\gamma \cos\theta}{d_e}, \qquad [2]$$

where P_p is the threshold capillary pressure required for nwp to enter a duct of effective diameter (d_e) with fluids having interfacial tension (γ) and contact angle (θ). P_{nw} is pressure in the nwp and P_w is pressure in the wp. Small increases or decreases of P_p cause the interface to advance or retreat in a reversible manner with piston-type motions.

In a duct of rectangular cross section, with width x and depth y, the threshold capillary pressure for $\theta_R = \theta_A = 0$ is given by

$$P_p = F(\epsilon)2\gamma\left(\frac{1}{x} + \frac{1}{y}\right), \quad \epsilon = \frac{x}{y}$$

$$F(\epsilon) = \frac{\epsilon(4 - \pi)}{2(1 + \epsilon)\{(1 + \epsilon) - [(1 + \epsilon)^2 - \epsilon(4 - \pi)]^{1/2}\}}. \qquad [3]$$

The dimensionless term $F(\epsilon)$ is nearly equal to 1 (4) and Eq. [2] can be approximated (10)

$$P_p = 2\gamma\left(\frac{1}{x} + \frac{1}{y}\right)\cos\theta \qquad [4]$$

for any value of θ.

From Eqs. [2] and [3] an effective diameter can be obtained,

$$d_e = \frac{2}{F(\epsilon)\left(\frac{1}{x} + \frac{1}{y}\right)} \qquad [5]$$

since both x and y are known. In our previous work (6), in experiments where pressures were measured and θ, γ, x, and y were all known, we found that d_e obtained from Eq. [5] satisfied Eq. [2]. Consequently the effective diameters of pores can be calculated using Eq. [5] and measured values of width (x) and depth (y).

In order for snap-off in a throat to cause trapping in a pore, the snap-off event must be on the downstream side of the pore. Thus, the aspect ratio for each pore was computed as the ratio of d_e for the pore to d_e for the downstream throat. These values are from ~1.3 to 2.0, in the models with low aspect ratio pores, and from ~2.3 to 2.8 in the high aspect ratio models. A model with "intermediate" aspect ratio pores was added for air–mercury experiments, the aspect ratio values of which are from ~1.8 to 2.4.

III. EXPERIMENTAL METHODS

An experiment commenced with the model filled with wp. Wetting phase was displaced from the sink chamber (Fig. 2) by nwp. Capillary pressure was then gradually increased and the sequence in which throats and pores were filled by nwp was recorded. This provides a check on the independently measured sizes. Drainage was complete when all pores and throats were filled with nwp. Wetting phase pressure was then increased or nwp pressure decreased slowly and the sequence in which nwp withdrew from throats and pores and the sequence and locations of snap-off and break-off events were recorded. At the end of imbibition, all of the nwp was disconnected and the location and amount of residual nwp recorded. Some pores were completely filled with trapped nwp and others only partially filled. In the latter case, the position of nwp within the pore also was recorded.

Drainage–imbibition experiments were performed for four fluid pairs with differing advancing and receding contact angles as shown in Table II. All contact angles are recorded as measured in the wetting phase. Static angles (θ_I) were measured in cylindrical glass tubes of accurately measured bore using

$$\theta = \text{arc sin}\left(\frac{b^2 - 4h^2}{b^2 + 4h^2}\right),$$

where θ is contact angle, b is the diameter of the tube bore, and h is the distance from the midpoint of a chord, which joins the points of fluid contact with the tube walls, to the fluid interface at the midpoint of the bore. This measurement avoids distortions of angle due to refraction. The nonwetting phase is contained as a static blob with equal contact angles at either end and no pressure gradient in the wetting phase.

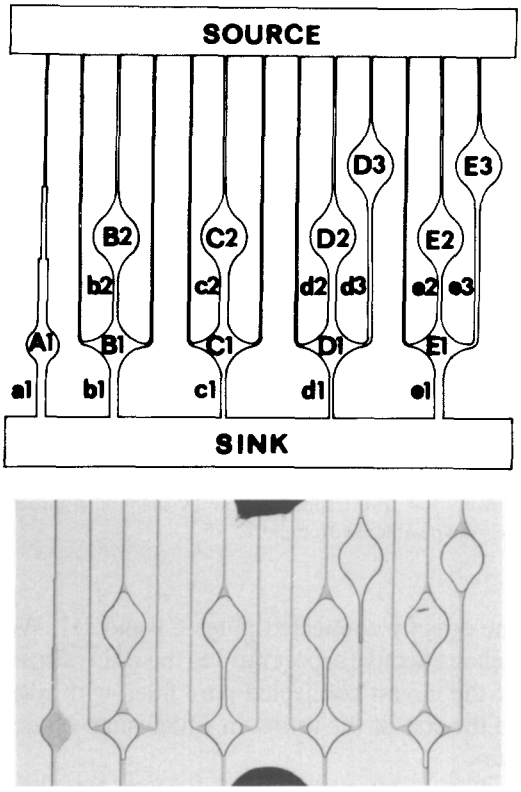

FIG. 5. Low aspect ratio, concave pore model at residual nwp saturation. Wetting phase darker, nonwetting phase lighter.

Advancing and receding contact angles were calculated from measured capillary pressures knowing the effective diameter of a duct and the interfacial tension of the fluids (6). Interfacial tension was measured by the drop-weight technique.

Glass surfaces were used either clean or with a thin coating of silicone and fluid pairs and surface conditions were chosen to give a wide range of contact angles (Table II). Preparation of the silicone-coated surface is described in (6).

IV. RESULTS

In the introduction we classified mechanisms of interface movement and displaced phase trapping. In this section we show how trapping is affected by the relative size, arrangement, and connectivity of pores and throats.

a. Snap-off in Throats

Figure 5 illustrates the low aspect ratio, concave-pore model at residual nwp saturation. Initially, the model was saturated with water (colored) and capillary pressure was increased until all throats except No. 1 (Fig. 3) were completely filled with nwp (air). The order of filling (drainage) is given in Table III and is in order of decreasing size of throats except for minor size discrepancies and for c2 and d2 where filling (drainage) was delayed related to lack of accessibility because of

TABLE III

Order of Drainage and Imbibition Events, Low Aspect Ratio Concave Pore Model

Drainage											
Throat	e1	a1	b1	d1	e2	(d2)	c1	(c2)	e3	b2	d3
Order of nwp entry	1	2	3	4	5	6	7	8	9	10	11
Effective throat diam. (d_e)	370	375	353	326	328	(347)	324	(351)	325	313	316
Imbibition											
Throat	d3	b2	e2	c1	e3	d1	b1	e1	c2	d2	a1
Order of snap-off	1	2	3	4	5	6	7	8	NS[a]	NS	NS
Effective throat diam. (d_e)	316	313	328	324	325	326	353	370	351	347	375

[a] No snap-off.

smaller throats c1 and d1 in series. Capillary pressure (P_c) was then reduced and during imbibition all interfaces in the smallest throats (size 1, Fig. 3) moved with piston-type motions to associated pores without rupture of nwp ($\theta_A = 0$). Further decreases of P_c caused snap-off in throats (sizes 2 and 3) in the order shown in Table III. This is an order of increasing size except for minor size discrepancies. Residual nwp is seen in Fig. 5.

Snap-off could not occur in throats c2 or d2 because snap-off had already disconnected nwp in the downstream throats c1 and d1 and trapped nwp in pores C1, D1, C2, and D2. Snap-off can occur only if nwp is continuous to a downstream sink. Since pores C2 and D2 both have greater than critical aspect ratio with respect to their downstream throats c2 and d2, respectively, it follows that a pore can have greater than critical aspect ratio with respect to directly connected throats yet snap-off does not occur in these throats. Thus, for throats directly connected to a particular pore, a greater than critical aspect ratio is a necessary but not sufficient condition for snap-off in those throats.

The "effective aspect ratios" for snap-off in throats c1 and d1 should be calculated with respect to the pores C2 and D2 rather than the directly connected pores C1 and D1. We define effective aspect ratio as the ratio of sizes of the largest connected pore filled with nwp to the size of the throat in which snap-off occurs.

If pore C1 and D1 had been of less than critical aspect ratio with respect to their downstream throats (c1 and d1) snap-off would still have occurred in c1 and d1 provided that the diameter ratios C2/c1 and D2/d1 were greater than critical. Thus, a pore could have all directly connected throats of less than critical aspect ratio and yet trap nwp by snap-off in one of these throats.

Nonwetting phase was trapped by snap-off in all pores with effective aspect ratios of 1.48 or larger (Table IV) indicating that this must be near to the critical aspect ratio for zero advancing contact angle (water–air system on clean glass).

Similar experiments performed in the high aspect ratio convex pore model showed that snap-off in throats can occur at a static contact angle of up to 63° (Fig. 7). A pyridine–water mixture (dark wp) displaced air (light nwp) in a glass model with silicone coated surfaces. Snap-off in throats caused trapping of nwp in all pores except for pore A. Table V gives the effective aspect ratio for all pores in this model

TABLE IV

Effective Aspect Ratios and Trapping, Low Aspect Ratio Concave Pore Model

Pore	Effective diameters		Effective aspect ratio	T or W
	Pore	Throat		
A1	530	375(a1)	1.41	W
B1	523	353(b1)	1.48	T
E1	528	370(e1)	1.43	T
B2	527	313(b2)	1.68	T
C2	527	324(c1)	1.63	T
D2	545	326(d1)	1.67	T
E2	538	328(e2)	1.64	T
D3	533	316(d3)	1.69	T
E3	534	325(e3)	1.64	T

Note. T = nwp trapped in pore by snap-off in throat; W = nwp withdrew from pore.

TABLE V

Effective Aspect Ratios and Trapping, High Aspect Ratio Convex Pore Model

Pore	Effective diameters		Effective aspect ratio	T or W
	Pore	Throat		
A1	564	240(a1)	2.35	W
B1	564	236(b1)	2.39	T
D1	554	221(d1)	2.51	T
E1	550	239(e1)	2.30	T
B2	567	222(b2)	2.55	T
C2	563	226(c1)	2.49	T
D2	565	239(d2)	2.36	T
E2	571	203(e2)	2.81	T
D3	560	204(d3)	2.75	T
E3	558	208(e3)	2.68	T

Note. T = nwp trapped in pore by snap-off in throat; W = nwp withdrew from pore.

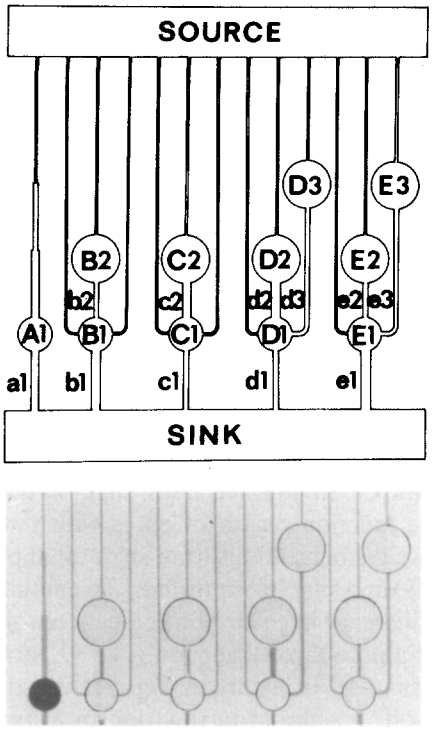

FIG. 6. High aspect ratio, convex pore model at residual nwp saturation. Wetting phase darker, nonwetting phase lighter.

and it is concluded that for a static contact angle (θ_I) of 63° the critical aspect ratio for snap-off in throats is between 2.35 and 2.39. In the experiment illustrated (Fig. 6), snap-off occurred in throat d2 before d1 although d2 is slightly larger. For a repeat experiment performed more slowly, d1 snaps-off before d2. Where contact angle is large but the size difference of throats is small (d1 = 221 μm, d2 = 239 μm), increases in the ratio of viscous to capillary forces favor earlier supply of wetting phase to upstream throats where snap-off occurs earlier than would be the case at lower flow rate.

Experiments were performed with four fluid pairs (Table II) having θ_I from 0° to 63° in four models of differing pore shape and aspect ratio. Data as in Tables III and IV were collected for each experiment. Effective aspect ratios r_p/r_t are recorded in Fig. 7 as a function of contact angle for pores in which nwp was trapped by snap-off in throats (crosses) and those in which nwp withdrew without trapping (solid circles). We also record experimental data previously obtained (6) in a different model with a single pore–throat pair (large open circles) where critical aspect ratio is plotted against advancing contact angle. These data for advancing angles (θ_A) compare closely with data for intrinsic angles (θ_I) from the present study and show that critical aspect ratio increases from ~1.5 to 1.75 for an increase in advancing contact angles from 0° to 55°. At higher values of θ_A, the critical aspect ratio increases more rapidly becoming infinitely large above ~70° (Fig. 7). Differences between the two curves are related to contact angle hysteresis.

b. Snap-off in Pores

Where effective aspect ratio is less than critical, snap-off occurs during imbibition either

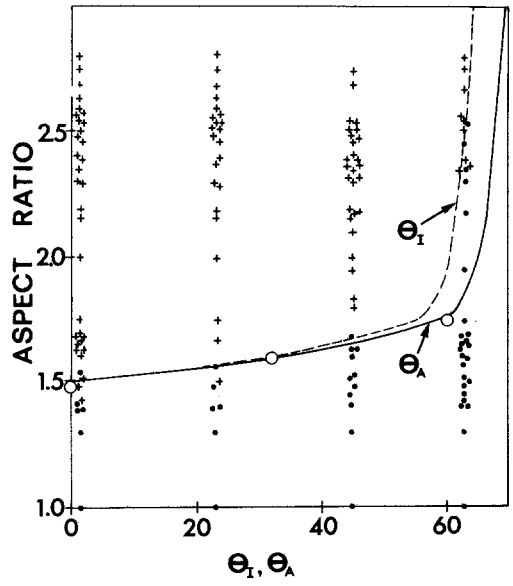

FIG. 7. Aspect ratio (pore-to-throat effective diameter ratio) as a function of static (θ_I) and advancing (θ_A) contact angles. Small crosses are experiments in which nwp was trapped by snap-off in throats and small solid dots experiments where snap-off in throats did not occur. Large open circles and solid line are from previous experimental study of snap-off in single pore–throat pair (6).

within pores or in the junction regions of pores and throats.

Figure 8 illustrates pores and throats of series D (Fig. 2) in the low aspect ratio concave-pore model. The fluid pair is a water–pyridine mixture (dark) displacing air (nonwetting) on silicone-coated glass ($\theta_I = 63°$). Wetting liquid interfaces advance (A) with piston-type motions from both left and right throats and a selloidal bridge of nwp extends through pore D1, becomes unstable and snaps-off *in the pore* (Figs. 8B and C) with little trapping of nwp (Fig. 8C). Pore D2 partially emptied before disconnection occurred.

The capillary pressure at which snap-off occurs in a pore is slightly lower than the capillary pressure for piston-type withdrawal from the same pore body. Piston-type withdrawal could not occur in this case because of the simultaneous advance of two interfaces from opposite throats. That is, whether piston-type withdrawal or snap-off can occur in a pore is also a matter of topology and fluid distribution. This is further explained in the following section.

c. *Snap-off at Pore–Throat Junctions*

For the model discussed in the previous section, air (wp) advances to displace mercury (nwp) (dark) on clean glass with $\theta_I = 45°$ (Fig. 9). Snap-off occurs at the pore-throat junction. Figures 9A, B, and C illustrate differences in interface form which arise from wp advance from only one adjacent throat (A), from two opposite throats (B), and from two adjacent throats (C). In all three cases, snap-off occurs at the junction region of pores with throats and we distinguish this from snap-off in pores (Fig. 8) and snap-off in throats. To emphasize the difference in collar position between snap-off at a pore-throat junction (Fig. 9A, arrow) and snap-off in a throat, Fig. 9D illustrates snap-off in a throat (arrow) for an air/water fluid pair. In all cases, there is partial trapping of nwp.

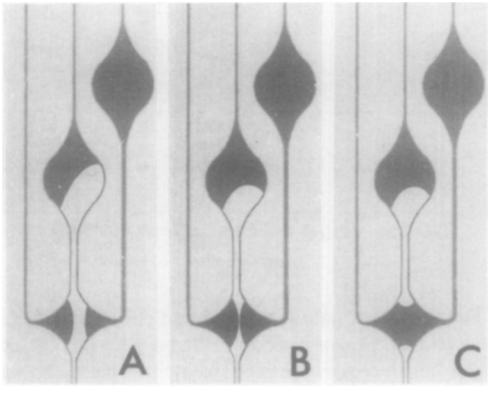

FIG. 8. Pores and throats of series D (Fig. 2) in low aspect ratio; concave pore model. A, B, and C show sequential interface positions with snap-off in pore.

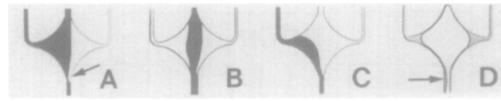

FIG. 9. Differences in interface form (air–mercury) arising from wp advance from only one adjacent throat (A), from two opposite throats (B) and from two adjacent throats (C) with snap-off events at pore–throat junctions (arrow in A) in all cases. D shows position of wp collar for snap-off in throat for comparison.

Previously, we defined critical aspect ratio as the pore–throat size ratio such that snap-off occurs in the throat at a capillary pressure higher than required for piston-type withdrawal from an associated pore. As noted in Section I, it is equivalent to the ratio of the capillary pressure required for piston-type withdrawal from a duct of given effective diameter to the capillary pressure required for snap-off in the same duct.

We now consider the ratio of the capillary pressure for piston-type withdrawal *from a pore* to the capillary pressure for snap-off *in that pore.* This ratio is 1.5 for θ_A equal to zero and corresponds with the critical aspect ratio for snap-off in throats. However, for contact angles of 20° or more, the ratio is ~1.03 (Fig. 10). That is, the capillary pressure for piston-type withdrawal from a pore is only slightly higher than for snap-off in the same pore. These capillary pressure ratios were obtained, not by direct measurement of pressures at the moment of snap-off but by recording the se-

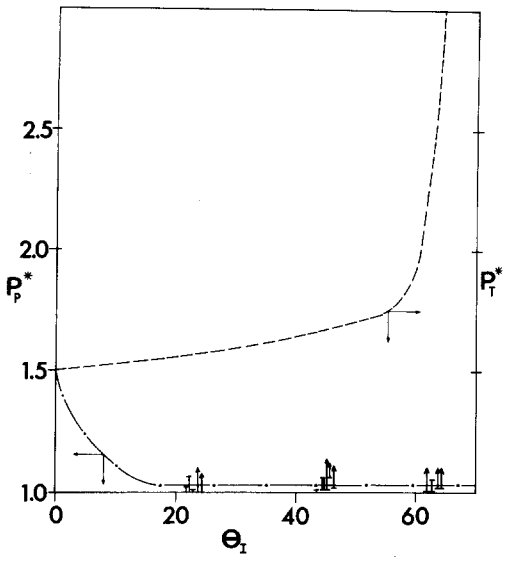

FIG. 10. Dash-dot line is relationship of imbibition capillary pressure for piston-type withdrawal from pore to capillary pressure of snap-off within pore, or at pore–throat junction (i.e., $P_p^* = P_{pp}/P_{sp}$), as a function of intrinsic contact angle. Broken line is for snap-off in throats transferred from Fig. 7 ($P_t^* = P_{pt}/P_{st} \equiv$ aspect ratio $= r_p/r_t$).

quence of snap-off in pore or at pore throat junction events in relation to snap-off in throat events and withdrawal from pore events and accurately knowing the effective diameters of all pores and throats. In some cases, the event of interest can be bracketed with lower and upper capillary pressure limits whereas, for other events, only a lower capillary pressure limit or only an upper capillary pressure limit could be obtained. These situations are recognized, respectively, as vertical bars with cross pieces on both ends, bars with upward pointing arrows and bars with cross pieces on the upper ends only (Fig. 10). For comparison, the ratio of piston-type withdrawal capillary pressure to snap-off capillary pressure for throats is transferred from Fig. 7 and shown as a broken line.

The importance of topology is illustrated schematically in Fig. 11 where the pores are conceived as spherical and the throats cylindrical. Suppose that pore-to-throat diameter ratios for A/a and B1/b1, B2/b2, and B/b are all less than critical so that no pore has a directly connecting throat small enough to exceed the critical aspect ratio. However, suppose the effective aspect ratios B1/a, B2/a, and B/a are all greater than critical for snap-off in throats. In the left portion of the diagram, as P_c decreased there was piston-type advance of convex interfaces from throats c1 and c2 to pores B1 and B2. Then, at a capillary pressure higher than required for piston-type withdrawal from these pores, snap-off occurred in throat "a" causing trapping in pores A, B1, B2 as well as in throats b1 and b2. Had the aspect ratios B1/b1 and B2/b2 been greater than critical, the outcome would have been the same. Throat "a" is smaller than b1 or b2 and snap-off occurs in "a" first eliminating the possibility of subsequent snap-off in b1 or b2.

In the right portion of the diagram, piston-type withdrawal of convex interfaces occurred in throats c1 and c2 and continued into pore A where a selloidal interface formed and snap-off followed at the junction of pore A with throat "a." Following snap-off, convex interfaces withdraw along throat "a" leaving pore A partially empty and throat b and pore B with trapped residual nwp. This illustrates that whether nwp is trapped in pore A depends not only on the relative size of the throat on the downstream side but the relative sizes and positions of throats and pores on the upstream side. The snap-off at pore–throat junction, in the right-hand case, would occur at a higher

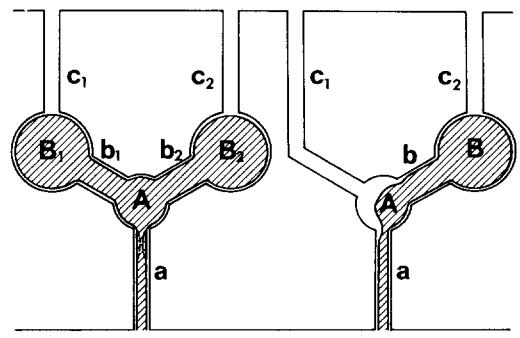

FIG. 11. Diagrammatic to illustrate effect of topology as well as pore–throat size on trapping. nwp is shaded.

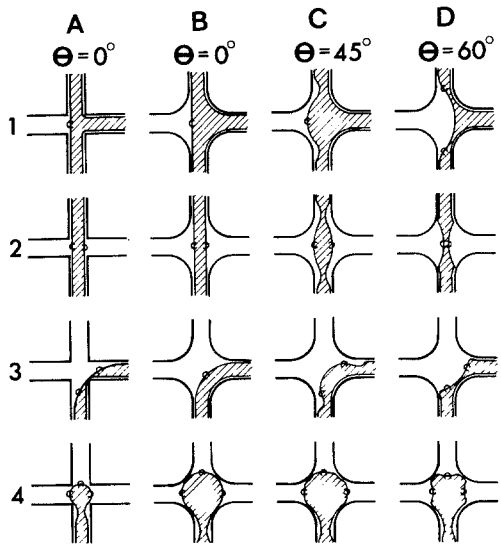

FIG. 12. Summary of experimental observations on effects of contact angle on interface shape and snap-off sites. nwp connects to pore from three throats, two opposite throats, two adjacent throats, and one throat only in 1, 2, 3, and 4, respectively.

capillary pressure than the snap-off in the throat in the left-hand case assuming similar fluids and sizes for A and a.

Further effects of topology are summarized in Fig. 12 from observations made in the concave pore model. The interface forms and break-off and snap-off events for various directions of wetting phase advance, aspect ratio and contact angle are given. It must be remembered that the dimensions of these pores and throats is much larger in the plane of the page than in a perpendicular direction.

A1, A2, and A3 are for strongly wetted systems of less than critical aspect ratio and were the subject of experimentation by Lenormand and others (4). In A1, piston-type withdrawal occurred from the left throat and in A2 from the left and right throats and the configurations illustrated are stable because of the small aspect ratio. A3 illustrates an unstable interface jumping and disconnecting by break-off. A4 illustrates the formation of a selloidal collar. If aspect ratio is less than critical, piston-type withdrawal occurs. If greater than critical, snap-off occurs in the throat with trapping in the pore.

Series B, C, and D, 1 to 3, all have throats with less than critical aspect ratio. Interface shapes are illustrated at similar capillary pressures and vary with contact angle. The snap-off capillary pressures for B1, B2, and B3 are lower than for C and D which is why the interfaces in B are illustrated before acquiring selloidal form. There is little or no trapping of nwp in pores in which snap-off has occurred within the pore or at the pore–throat junction; however, the associated disconnection of nwp may isolate and trap nwp in adjacent pores and throats.

For A4, B4, C4, and D4, if the pores have aspect ratios less than critical with respect to the outlet throat, there is simple piston-type withdrawal. If the aspect ratio is greater than critical, snap-off occurs in the throat with nwp trapping in the pore.

These examples illustrate the importance of the relative size and position of throats, the initial distribution of phases and wettability on the position of snap-off sites and the amount of trapped nwp in pores.

V. DISCUSSION AND CONCLUSIONS

During imbibition from initial high nwp saturations, interfaces in throats move into adjacent pores by piston-type motions and break-off and snap-off events disconnect nwp and provide new interfaces in throats which undergo further piston-type motions. In the early stages of displacement, local disconnection of nwp facilitates further withdrawal of nwp but, as the displacement progresses, the probability increases that snap-off events will cause complete disconnection and trapping of domains of nwp.

Both break-off and snap-off occur during unstable interface jumps but for break-off the interfaces are convex whereas for snap-off interfaces are selloidal and have components of negative as well as positive curvature. Break-off occurs in pores with aspect ratios less than critical and with local constraints of shape such

that a convex interface impinges on an opposing pore wall and ruptures.

Most disconnection of nwp during imbibition probably occurs by one of several types of snap-off. The critical aspect ratio necessary for snap-off in throats is 1.5 for θ_A equal to zero and increases only slightly to 1.75 for θ_A equal to $\sim 55°$. Thus, snap-off in throats is not a very sensitive function of θ_A within this range of contact angles. Above 70°, snap-off in throats cannot occur during quasistatic displacement where there is equilibrium of capillary pressure between pores and throats. For a pore and a throat of similar cross-sectional shape, critical aspect ratio (r_p/r_t) is equal to the ratio of the capillary pressure for piston-type withdrawal from *this throat* to the snap-off capillary pressure *in the same throat,* i.e., P_{pt}/P_{st} which we have designated as the critical capillary pressure ratio for snap-off in throats (P_t^*).

Snap-off is possible in pores or at pore–throat junctions at capillary pressures only slightly less than required for piston-type withdrawal from the pore bodies ($P_{pp}/P_{sp} \cong 1.03$) except for cases where $\theta < 20°$. This capillary pressure ratio (P_{pp}/P_{sp}) is designated as the critical capillary pressure ratio for snap-off in pores (P_p^*). P_p^* and P_t^* are for constant cross sectional shape of pores and throats and constant wettability.

Snap-off in a pore or at a pore–throat junction commonly leaves the host pore with only small amounts of trapped nwp. However, these events, as is the case for snap-off in throats, may disconnect associated pores which can remain completely filled with trapped nwp. Snap-off in throats traps nwp in directly connected upstream pores and the degree of filling will increase with increasing aspect ratio.

Trapping of nwp is influenced by topology. The concept of effective aspect ratio relates the relative sizes of pores and throats which are effective in allowing snap-off whether or not they are in direct contact. A pore can have greater than critical aspect ratio with respect to all directly connected throats and yet snap-off not occur in those throats. Conversely, a pore can have less than critical aspect ratio with respect to all directly connected throats and yet snap-off occur in those throats. Also, whether interfaces arrive in pores from one throat or simultaneously from several connected throats affects the subsequent interface motion through the pore and the location of snap-off sites. Thus, effective aspect ratio is influenced by wettability, size, shape and arrangement of pores and throats (topology) and distribution of fluid phases with respect to source and sink.

The amount and location of residual nwp depends on the sequence of local interface movements as pressure is lowered. From the foregoing we can deduce the sequence of events leading to disconnection of nwp during imbibition in a network of pores and throats of any size. Consider capillary pressure falling from P_{c1} to P_{c2}. The possible events can be tabulated as follows. Assuming continuity of nwp to the sink:

1. For any throat,
   - A. if d_e throat $\leqq (1/P_t^*)\ 4\gamma \cos\theta_A/P_{c2}$, snap-off occurs in the throat. P_t^* is the critical capillary pressure ratio for throats (see Sect. 1 and Fig. 10, broken line).
   - B. if d_e throat $> (1/P_t^*)\ 4\gamma \cos\theta_A/P_{c2}$, a stable nwp bridge with a finite neck diameter develops in the throat.
2. For any pore,
   - A. if only one directly connected throat contains nwp, complete, piston-type withdrawal occurs if,
     $d_e$pore $\leqq 4\gamma \cos\theta_A/P_{c2}$.
   - B. if more than one, but less than all, directly connected throats are occupied by nwp,
     - (i) snap-off occurs in the pore or at the pore–throat junction when $d_e \leqq (1/P_p^*)\ 4\gamma \cos\theta_A/P_{c2}$, where P_p^* is the critical capillary pressure ratio for snap-off in pores (see Sect. 1). The dash-dot line on Fig. 10 gives the relationship of P_p^* to θ_1

and this will be closely similar to the relationship of P_p^* to θ_A. For $\theta_I > 20°$, P_p^* is insensitive to changes of angle and for $\theta_I < 20°$, contact angle hysteresis is small.

(ii) break-off will occur as a result of certain pore shape constraints at approximately the same capillary pressure as snap-off in pores.

C. if $d_e\text{pore} > 4\gamma \cos \theta_A / P_{c2}$, there is partial withdrawal of the interface from the pore, including adjustment of thin-film thickness.

If any snap-off or break-off events cause nwp continuity to be broken, nwp becomes trapped.

In conclusion, drainage capillary pressures are mainly bond (throat)-controlled whereas this study and others (4) show that imbibition is both bond- and site (pore)-controlled. Interface movements during imbibition are influenced by the sizes, shapes, and arrangement of both pores and throats with respect to the direction of advancing displacing phase. Earlier interface motions determine what is possible subsequently and the sequence and position of snap-off and break-off events determine the amount and location of trapped nonwetting phase. Wettability and topology are the main factors which determine whether snap-off occurs in throats, in pores, or at pore–throat junctions. Wherever it occurs, the effect is to disconnect nonwetting phase and, ultimately, to cause its entrapment.

ACKNOWLEDGMENTS

Financial assistance from the Government of the People's Republic of China and a grant in aid of research from the Natural Sciences and Engineering Research Council of Canada are gratefully acknowledged. Dr. W. G. Laidlaw, Dept. of Chemistry, University of Calgary, critically read the manuscript and made several important observations which have led to its improvement. Mr. W. Tang Kong prepared the illustrations and Ms. M. Boody typed the manuscript. We thank all of them for their assistance.

REFERENCES

1. Melrose, J. C., and Brandner, C. F., *J. Canad. Pet. Technol.* **13,** 54 (1974).
2. Mohanty, K. K., Davis, H. T., and Scriven, L. E., *in* "Surface Phenomena in Enhanced Oil Recovery" (D. O. Shah, Ed.), p. 595. Plenum, New York, 1981.
3. Mohanty, K. K., Davis, H. T., and Scriven, L. E., *Soc. Pet. Eng.*, 9406 (1980).
4. Lenormand, R., Zarcone, C., and Sarr, A., *J. Fluid Mech.* **135,** 337 (1983).
5. Roof, J. G., *Soc. Pet. Eng. J.*, **10,** 85 (1970).
6. Li, Y., and Wardlaw, N. C., *J. Colloid Interface Sci.* **109,** 461 (1986).
7. Lai, F. S. Y., "Reduction of the So-called "Irreducible" Wetting Phase Situation—A Study Using Water-Wet and Oil-Wet Transparent Micromodels and Sandstone Samples," Ph.D. thesis. University of Waterloo, Waterloo, Ontario, 1984.
8. McKellar, M., and Wardlaw, N. C., *J. Canad. Pet. Technol.*, 21 (1982).
9. Bell, W. K., van Brakel, J., and Heertjes, P. M., *Powder Technol.* **29,** 75 (1981).
10. Lenormand, R., and Zarcone, C., *Soc. Pet. Eng.* 13 264 (1984).